

SCIENTIFIC REPORTS



OPEN

Inflammatory Eicosanoids Increase Amyloid Precursor Protein Expression via Activation of Multiple Neuronal Receptors

Katie J. Herbst-Robinson^{1,*}, Li Liu^{1,*}, Michael James¹, Yuemang Yao¹, Sharon X. Xie² & Kurt R. Brunden¹

Received: 24 April 2015
Accepted: 26 October 2015
Published: 17 December 2015

Senile plaques comprised of A β peptides are a hallmark of Alzheimer's disease (AD) brain, as are activated glia that release inflammatory molecules, including eicosanoids. Previous studies have demonstrated that amyloid precursor protein (APP) and A β levels can be increased through activation of thromboxane A₂-prostanoid (TP) receptors on neurons. We demonstrate that TP receptor regulation of APP expression depends on G α_q -signaling and conventional protein kinase C isoforms. Importantly, we discovered that G α_q -linked prostaglandin E₂ and leukotriene D₄ receptors also regulate APP expression. Prostaglandin E₂ and thromboxane A₂, as well as total APP levels, were found to be elevated in the brains of aged 5XFAD transgenic mice harboring A β plaques and activated glia, suggesting that increased APP expression resulted from eicosanoid binding to G α_q -linked neuronal receptors. Notably, inhibition of eicosanoid synthesis significantly lowered brain APP protein levels in aged 5XFAD mice. These results provide new insights into potential AD therapeutic strategies.

A key pathological feature of the Alzheimer's disease (AD) brain is the presence of senile plaques comprised of A β peptides, which are proteolytically-derived from the amyloid precursor protein (APP)¹. These plaques are thought to contribute, either directly or indirectly, to the neuronal dysfunction and dementia associated with AD². Other factors that are believed to contribute to AD pathogenesis include intracellular aggregates of hyperphosphorylated tau protein³, oxidative stress⁴, and neuroinflammation⁵.

The inflammation observed in AD brain results largely from increased microglial activation in the vicinity of senile plaques^{6,7} and a number of glial-derived inflammatory molecules, including cytokines, chemokines and eicosanoids, as well as oxidizing molecules, have been suggested to exacerbate AD neuropathology^{5,8}. For example, isoprostane F_{2 α} III (iPF_{2 α} III), a lipid oxidation product thought to be elevated in AD brain^{9,10}, can activate the thromboxane A₂ (TXA₂)-prostanoid (TP) receptor on neurons with a resulting increase of APP mRNA stability that leads to enhanced APP expression and A β production^{11,12}. Similarly, TXA₂ itself may also be increased in AD brain, as this eicosanoid is produced by activated microglia¹³.

The signaling pathways that underlie the conversion of TP receptor activation into increases of APP expression and A β production have not been previously explored, and here we demonstrate the involvement of G α_q and conventional PKC isoforms. Importantly, we have discovered that activation of additional eicosanoid receptors, including those that bind prostaglandin E₂ (PGE₂) and leukotriene D₄ (LTD₄), also results in increased APP levels in receptor-transfected cells, as well as in primary rat or mouse neurons. As PGE₂, TXA₂, and LTD₄ can be released from microglia^{5,14}, with the former shown to be elevated in the cerebrospinal fluid of AD patients^{15,16}, these studies further implicate glial inflammation in the pathogenesis of AD. An assessment of 5XFAD transgenic mice that develop A β plaques revealed an age-dependent elevation of PGE₂ and TXA₂, as well as APP. Importantly, inhibiting eicosanoid synthesis in aged 5XFAD mice led to significant diminutions of total APP levels and of

¹Department of Pathology and Laboratory Medicine, Center for Neurodegenerative Disease Research, Perelman School of Medicine, University of Pennsylvania, Philadelphia, Pennsylvania 19104-6323, USA. ²Department of Biostatistics and Epidemiology, Perelman School of Medicine, University of Pennsylvania, Philadelphia, Pennsylvania 19104-6323, USA. *These authors contributed equally to this work. Correspondence and requests for materials should be addressed to K.R.B. (email: kbrunden@upenn.edu)

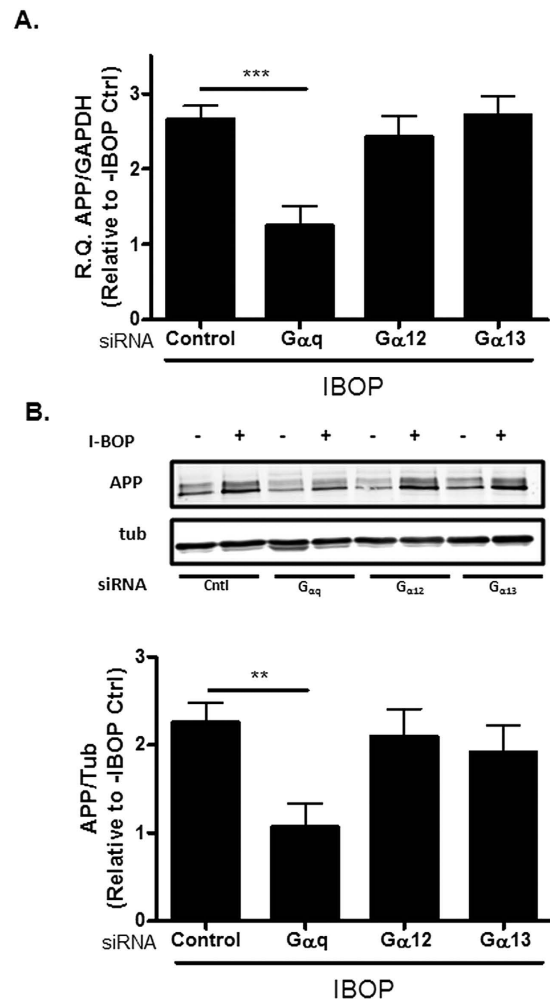


Figure 1. Knockdown of G α_q inhibits TP receptor-mediated increases in APP and A β . hTP-hAPP cells were transfected with 50 nM of control siRNA or siRNA directed to G α_q , G α_{12} , or G α_{13} and cultured for 72 h, with IBOP (10 nM) added over the last 48 h. **(A)** qRT-PCR analysis revealed a reduction in IBOP-induced APP mRNA levels only in cells treated with G α_q siRNA [R.Q. (relative quantification) values of APP/GAPDH from qPCR are plotted relative to non-IBOP-treated cells without siRNA addition]. **(B)** Only cells treated with G α_q siRNA showed reduced APP protein expression, as determined by immunoblot analysis with 5685 antibody [values are relative to non-IBOP-treated cells without siRNA addition, with normalization to α -tubulin]. Statistical analyses consisted of a mixed-effects model, with values representing estimates from the least squares means fit of the mixed procedure from 2–6 independent studies with 1–3 replicates for each treatment/study. Error bars represent SEM; ** $p < 0.01$; *** $p < 0.001$.

α - and β -secretase processed COOH-terminal fragments of APP. The results of these studies provide important new insights into the regulation of APP in the AD brain.

Results

TP Receptor Regulation of APP and A β Synthesis is Dependent on G α_q and Conventional PKC Isoforms. To investigate the intracellular signaling molecules involved in the previously reported TP receptor-induced increases in APP expression and A β production that result from APP mRNA stabilization^{11,12}, we utilized siRNA directed to G α_q , G α_{12} , and G α_{13} , the G-protein α -subunits most commonly implicated in TP receptor signal transduction¹⁷. QBI293 cells stably expressing both the human TP receptor (hTP) and human APP₆₉₅ (hTP-hAPP cells) were transfected with control siRNA or siRNA directed to each of the three G-proteins and incubated for 24 h, followed by 48 h treatment in the presence or absence of the TP receptor agonist, [1S-1 α ,2 β (5Z),3 α (1E,3R*),4 α)]-7-[-3-(3-hydroxy-4-(4''-iodophenoxy)-1-butenyl)-7-oxabicyclo-[2.2.1]heptan-2-yl]-5-heptenoic acid (IBOP). In agreement with prior studies^{11,12}, IBOP caused a 2–3-fold increase in APP mRNA and protein in cells receiving control siRNA relative to non-IBOP treated cells (Fig. 1). A significant and nearly complete reduction of the IBOP-induced APP mRNA (Fig. 1A) and protein (Fig. 1B) was observed in cells transfected with siRNA directed to G α_q , and not in those that received G α_{12} or G α_{13} siRNA. There was a substantial knockdown of each of the G α mRNAs and corresponding proteins under these conditions (Supplementary Table 1).

$G\alpha_q$ involvement in promoting TP receptor-mediated increases in APP expression was further investigated by pre-incubation of IBOP-treated hTP-hAPP cells with the pan protein kinase C (PKC) inhibitor, Go6983¹⁸, to inhibit the activation of PKC downstream of $G\alpha_q$. Cells were also treated with the Rho-associated protein kinase inhibitor, Y-27632¹⁹, which blocks signaling downstream of $G\alpha_{12/13}$ activation²⁰. Only cells that were pretreated with Go6983 showed decreased APP mRNA, APP protein, and A β 1-40 (Supplementary Figure 1) following IBOP stimulation, whereas Y-27632 alone had no effect and its addition did not further increase the effect of Go6983. Although small amounts of A β 1-42 could be detected in the cellular medium, quantification was not reliable. In conclusion, these studies demonstrate that TP receptor activation of $G\alpha_q$ results in increased levels of APP mRNA and protein, as well as increased production of A β .

As the addition of Go6983 revealed that one or more PKC species appeared to be key mediators of TP receptor regulation of APP expression, studies were conducted to examine which specific isoform(s) of PKC are critical to this pathway. There are three broad classes of PKCs²¹: conventional cPKC isoforms that are activated by Ca^{++} and diacylglycerol (DAG); novel nPKC isoforms that are activated by DAG, but are Ca^{++} -insensitive; and atypical PKC isoforms that are insensitive to both DAG and Ca^{++} , and are activated by other phospholipids. To determine which of the PKC classes are involved in the regulation of APP expression, hTP-hAPP cells were treated with the DAG mimic, phorbol 12-myristate 13-acetate (PMA)²², either alone or with the calcium ionophore, ionomycin (Iono)²³. A significant increase in APP mRNA (Fig. 2A) and protein (Fig. 2B), as well as in A β 1-40 production (Fig. 2C), were observed upon PMA treatment. The co-treatment of cells with PMA plus ionomycin induced a greater increase of APP mRNA and APP protein expression than was observed with PMA alone (Fig. 2A,B), and the effect of PMA alone or PMA plus ionomycin was blocked by Go6983. A similar trend was observed when A β 1-40 levels were monitored, although the ionomycin enhancement of the PMA effect was not clearly evident (Fig. 2C). The enhanced APP expression observed with the Ca^{++} ionophore in the presence of PMA suggests that it is primarily cPKC isoforms that are responsible for the effects on APP.

To further define the cPKC isoforms involved in the regulation of APP expression, select cPKC (α and β II) and nPKC (ϵ) isoforms were knocked down via siRNA in hTP-hAPP cells. Efficient knockdown of the PKC isoforms was observed 72 h after transfection (see Supplementary Table 2), and siRNA-treated cells were incubated in the presence of IBOP. Cells that were treated with siRNA directed against PKC ϵ showed no decrease in APP protein expression (Supplementary Figure 2) relative to cells receiving control siRNA. Conversely, transfection with siRNA directed against PKC α or PKC β II reduced the IBOP-induced increases in APP mRNA and protein, with PKC β causing a greater reduction. Simultaneous PKC α and PKC β II siRNA addition did not completely inhibit IBOP-induced increases in APP expression, perhaps due to the residual PKC α and PKC β II that remain after knockdown, or because an additional cPKC isoform also contributes partially to the regulation of APP expression. Nonetheless, these findings further confirm that cPKCs are largely responsible for the effects of TP receptor activation on APP expression.

Additional Eicosanoid Receptors Regulate APP Expression. The aforementioned findings raised the question of whether other $G\alpha_q$ -coupled receptors, in addition to the TP receptor, might also affect APP levels. In particular, the compelling evidence of a connection between neuroinflammation and AD pathology prompted an investigation of additional $G\alpha_q$ -linked receptors that, like the TP receptor, are reported to be expressed on neurons and can be activated by inflammatory eicosanoids. This led to an evaluation of the PGE2 receptors, EP1 and EP3²⁴, the LTD4 receptor, CysLT1²⁵, and the LTB4 receptor, BLT1²⁶. QBI293 cells stably-expressing hAPP were transfected with constructs encoding each of these receptors, and these cells were subsequently exposed to known agonists. Ligand activation of the EP1, EP3, and CysLT1 receptors, but not the BLT1 receptor, led to increases in APP mRNA (Fig. 3A) and protein (Fig. 3B), as well as A β (1-40) (Fig. 3C). In the case of the EP1 and EP3 receptor-expressing cells, some A β (1-40) was produced in the absence of agonist, presumably due to a constitutive receptor activity. The lack of APP increase after BLT1 transfection was not the result of poor receptor expression, as qPCR analysis revealed the presence of appreciable transcript (Supplementary Table 3). Thus, activation of multiple $G\alpha_q$ -linked eicosanoid receptors results in enhanced APP expression and A β release. However, this does not appear to be a feature of all $G\alpha_q$ -coupled receptors, as activation of the BLT1 receptor or the unrelated $G\alpha_q$ -linked angiotensin I receptor (not shown) did not result in changes of APP expression.

Each of the inflammatory eicosanoids that were found to increase APP expression were examined for their effects on primary rat hippocampal neuron cultures that were treated with an anti-mitotic (cytosine arabinoside) to deplete dividing, non-neuronal cells. Consistent with prior observations¹¹, IBOP addition resulted in a significant increase of APP (Fig. 4A) that could be blocked with the specific antagonist, CNDR-51280 [compound 5 in¹²]. Treatment of the neurons with LTD4 or the PGE2 analogue, 17PGE2, also led to increased APP expression (Fig. 4B-D). The LTD4-mediated increase of APP was effectively inhibited with the CysLT1 receptor antagonist, pranlukast²⁷ (Fig. 4B). Interestingly, the EP1 antagonist, ONO8711²⁸, did not block the 17PGE2-induced elevation of APP (Fig. 4C), whereas the EP3 antagonist, L798,106²⁹, significantly inhibited the effect of 17PGE2 on APP expression (Fig. 4D). These data thus imply that the EP3 receptor, but not the EP1 receptor, mediated the 17PGE2-triggered increase of APP expression in rat hippocampal neuron cultures.

The relative magnitude of the increase of APP expression in the rat neurons was similar upon activation of each of the eicosanoid receptors, suggesting a similar degree of intracellular signaling via cPKC isoforms. To examine this further, additional studies were conducted in which high concentrations of the receptor agonists were added singly, or concurrently, to rat hippocampal neuron cultures. The simultaneous addition of all three stimulatory eicosanoids did not increase APP expression beyond that observed when each of these agents was added individually (Fig. 5A). A similar observation was made with primary mouse cortical neuron cultures (Fig. 5B). Although the addition of saturating levels of multiple agonists to the eicosanoid receptors did not lead to additive increases of APP expression, concurrent treatment of rat hippocampal neurons with sub-saturating concentrations of IBOP and 17PGE2 resulted in an increase of APP expression relative to that obtained with each agonist added alone (Fig. 5C).

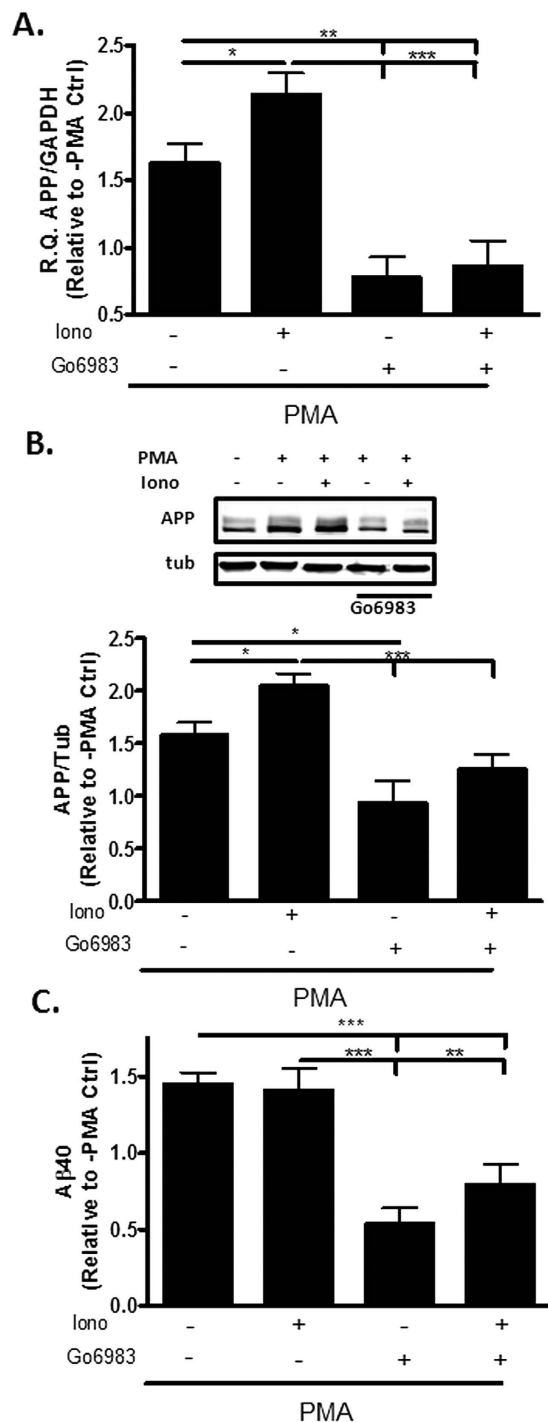


Figure 2. Phorbol ester and ionomycin treatment trigger increased APP expression. Treatment of QBI293 cells stably-expressing hAPP with PMA (1 μ M) for 36 h resulted in increased (A) APP mRNA [R.Q. values of APP/GAPDH are relative to vehicle-treated cells], (B) APP protein expression [(top) representative blot and (bottom) quantification of APP detected with 5685 antibody, with values relative to vehicle-treated cells and normalization to α -tubulin], and (C) A β 1-40 production [values are relative to vehicle-treated cells and normalized to total cellular protein content]. Addition of ionomycin (1 μ M) to PMA further increased APP mRNA and protein expression, and Go6983 treatment inhibited these increases. Statistical analyses consisted of a mixed-effects model, with values representing estimates from the least squares means fit of the mixed procedure from 2–4 independent studies with 2–5 replicates for each treatment/study. Error bars represent SEM; * $p < 0.05$; ** $p < 0.01$; *** $p < 0.001$.

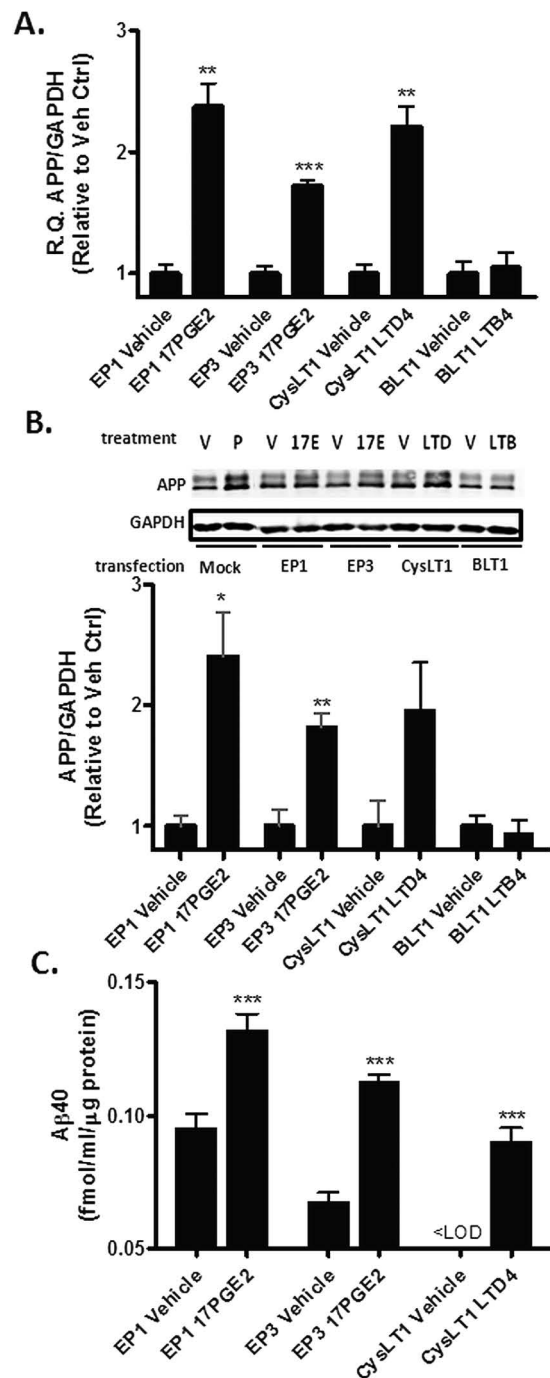


Figure 3. Additional $G\alpha_q$ -linked receptors regulate APP expression and $A\beta$ release. hAPP-expressing QBI293 cells were transiently transfected with cDNA encoding the human EP1, EP3, CysLT1 or BLT1 receptors. (A–C) The cells were treated for 36 h with vehicle or with agonist (100 nM 17PGE2 for EP1 and EP3; 1 μ M LTD4 for CysLT1; 1 μ M LTB4 for BLT1), followed by analysis of (A) APP mRNA [R.Q. values of APP/GAPDH are relative to vehicle-treated cells], (B) APP protein [(top) representative blot and (bottom) quantification of APP with 5685 antibody relative to the vehicle-treated cells, normalized to GAPDH], or (C) $A\beta$ 1-40 released into the culture medium. The presented data are the means obtained from a single independent study conducted with each treatment in triplicate. For $A\beta$ 1-40 ELISA determinations, each sample was analyzed in triplicate. A second independent study was conducted to confirm the findings (not shown). A two-tailed, t-test was applied to test if the values of the treatment groups differed relative to receptor-transfected cells in the absence of agonist. A one sample t-test was conducted in (C) for the CysLT1 samples, as the $A\beta$ 1-40 was below the level of detection in the vehicle group. Error bars represent SEM; * $p < 0.05$; ** $p < 0.01$; *** $p < 0.001$. <LOD = below limit of detection.

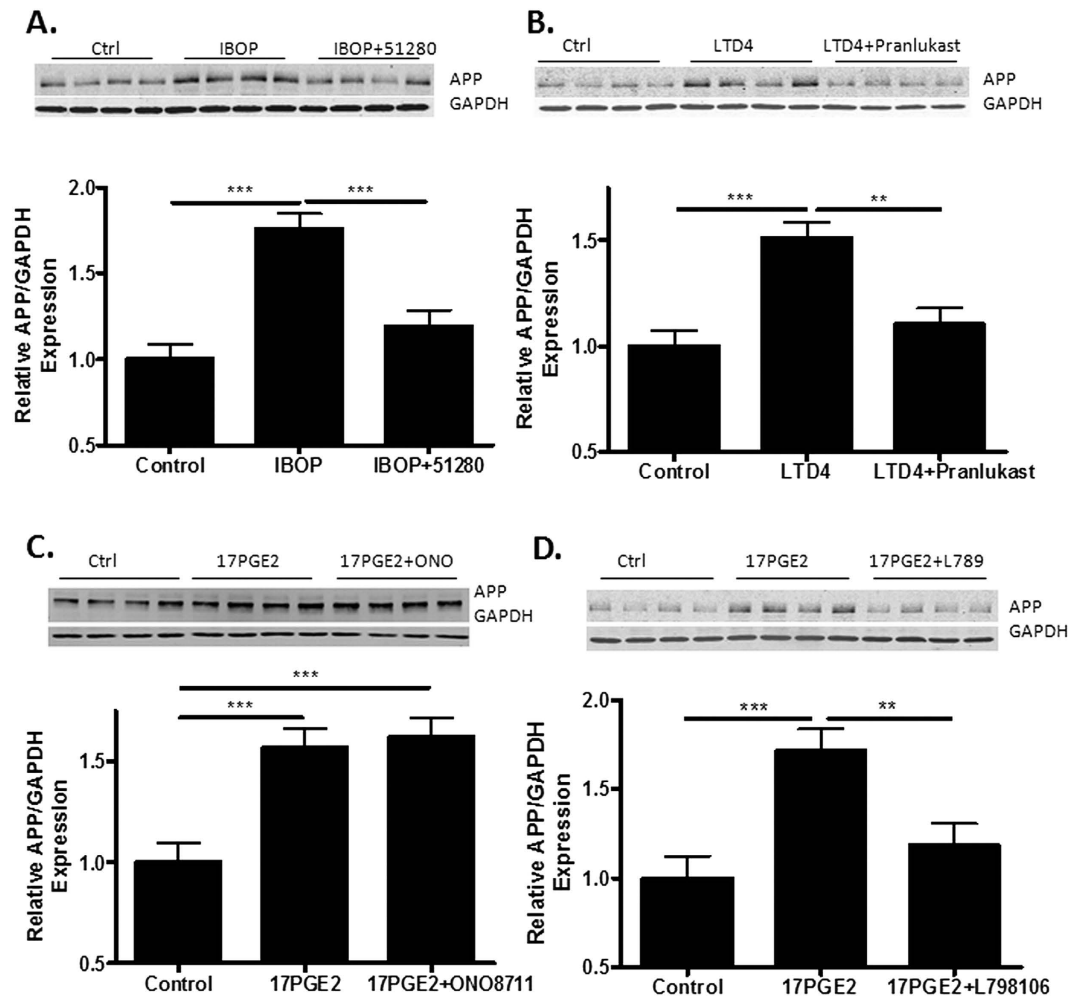


Figure 4. Activation of eicosanoid receptors increases APP expression in primary rat hippocampal neurons. Rat hippocampal neurons that were grown in culture for 14 days were treated for 2 days with receptor agonist alone or in combination with a specific receptor antagonist, and APP expression was compared to that of control cultures by immunoblotting (22C11 antibody). **(A)** IBOP (100 nM) increased APP expression and was blocked by the TP receptor antagonist, CNDR-51280 (10 μ M); **(B)** LTD4 (1 μ M) increased APP expression and was inhibited by the CysLT1 receptor antagonist, Pranlukast (1 μ M); and **(C,D)** 17PGE2 (1 μ M) enhanced APP expression, and was not inhibited by the EP1 receptor antagonist, ONO8711 (20 nM), but was blocked by the EP3 receptor antagonist, L798,106 (30 nM). Statistical analyses consisted of a mixed-effects model, with values representing estimates from the least squares means fit of the mixed procedure from 3 independent studies, with 4 replicates per study. Error bars represent SEM; ** $p < 0.01$; *** $p < 0.001$.

Evidence of Eicosanoid Enhancement of APP Expression in the 5XFAD Transgenic Mouse Model of AD.

The discovery that multiple eicosanoids could increase APP expression through interaction with neuronal receptors suggested that a vicious cycle may ensue in the AD brain, whereby initial glial activation by A β oligomers and/or plaques results in a release of inflammatory eicosanoids that subsequently up-regulate APP and A β production. PGE2 is reported to be elevated within the CSF of AD patients¹⁶, and to further explore whether there are increased eicosanoid levels in a mouse model with A β plaques, we measured both PGE2 and the TXA2 metabolite, TXB2, in 5XFAD transgenic mice in which robust A β deposition and glial inflammation are observed with age³⁰. The levels of PGE2 (Fig. 6A) and TXB2 (Fig. 6B) were comparable in brain homogenates from 1.5-month old 5XFAD transgenic mice and age-matched non-transgenic littermates, an age where the 5XFAD mice show relatively little A β deposition³⁰. In contrast, significant increases in these eicosanoids were observed in the brains of 6.5-month old 5XFAD mice, which have profound A β deposition³⁰, relative to age-matched non-transgenic mice and to the younger 5XFAD mice (Fig. 6A,B). Attempts were made to quantify LTD4 levels in 5XFAD mouse brain homogenates, but the amounts were below the level of detection by LC-MS/MS. The observation of an age-dependent increase of brain eicosanoids in 5XFAD mice suggested that there may be a comparable increase of APP expression in the older mice due to activation of neuronal receptors, as described above. Notably, total APP levels in the cortex and hippocampus were elevated approximately two-fold in 6-month old 5XFAD mice relative to younger mice (Fig. 6C and Supplementary Figure 3). The age-dependent increase in APP appeared to occur in both genders of 5XFAD mice, although the inclusion of only two female mice in both the 1.5- and 6-month

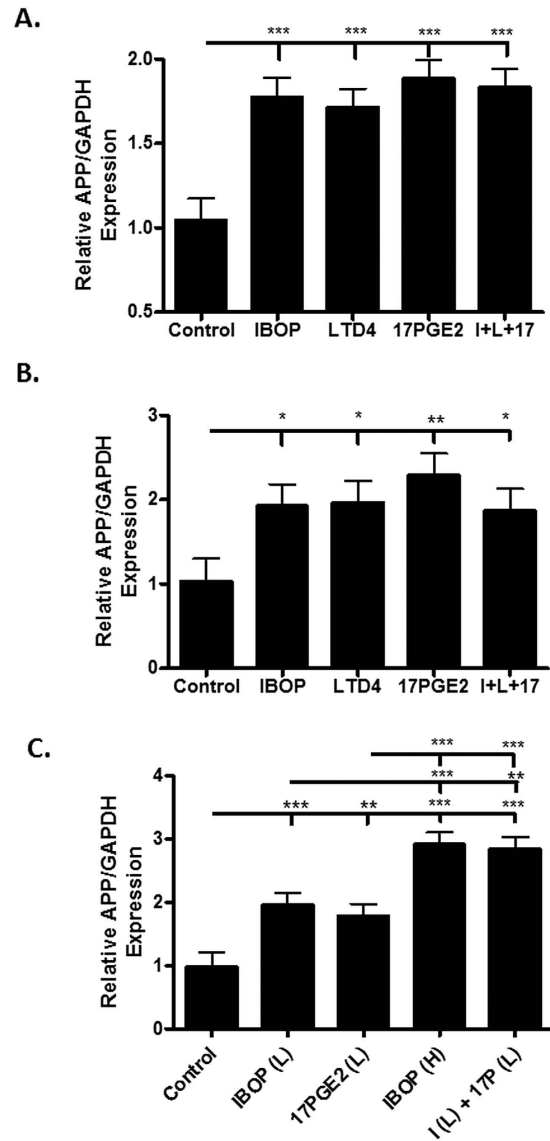


Figure 5. Activation of eicosanoid receptors in primary neurons with saturating and sub-saturating concentrations of receptor agonists. Rat hippocampal neurons (A) or mouse cortical neurons (B) that were grown in culture for 14 days were treated for 2 days with vehicle or high concentrations of IBOP (100 nM), LTD4 (1 μ M), 17PGE2 (1 μ M), or the combination of these agonists (I + L + 17). In (C), rat hippocampal neurons were treated with vehicle or sub-saturating concentrations of IBOP (50 nM; IBOP(L)), 17PGE2 (0.5 μ M; 17PGE2(L)), or the combination of these agonists (I(L) + 17(L)). In addition, neurons were also treated with a high concentration of IBOP (100 nM; IBOP(H)). APP was quantified from immunoblots (22C11 antibody), and statistical analyses consisted of a mixed-effects model, with values representing estimates from the least squares means fit of the mixed procedure from 3–4 independent studies, with 2–3 replicates per study. Error bars represent SEM; * $p < 0.05$, ** $p < 0.01$; *** $p < 0.001$.

old groups did not allow for a statistical comparison of age effect by gender. Interestingly, whereas a significant increase in APP levels was observed with antibodies that recognize α - and β -secretase cleaved APP (i.e., sAPP) as well as intact APP (Fig. 6C; 22C11 antibody and Supplementary Figure 3B; Karen antibody), the age-dependent elevation in APP was not observed when only intact APP was measured with a COOH-terminal antibody (Fig. 7 and Supplementary Figure 4; 5685 antibody). This suggested that there was an increase of sAPP in the older transgenic mice, and analysis of APP COOH-terminal fragments generated after α - and β -secretase cleavage of APP also revealed a significant increase in these fragments in the older 5XFAD mice (Fig. 7). Notably, both the larger COOH-terminal fragment, which should correspond to the C99 fragment generated after β -secretase cleavage of APP, and the smaller C83 COOH-terminal fragment that results from α -secretase cleavage of APP³¹, are increased in the older 5XFAD mice. This commensurate increase of sAPP and both α/β -secretase-generated COOH-terminal fragments of APP in the 6.0-month old 5XFAD mice suggests that there is an overall increase of APP expression in the older mice, with the majority of the increased APP undergoing processing, rather than an elevation of sAPP species that results from slowed sAPP degradation or a specific change in activity of one of

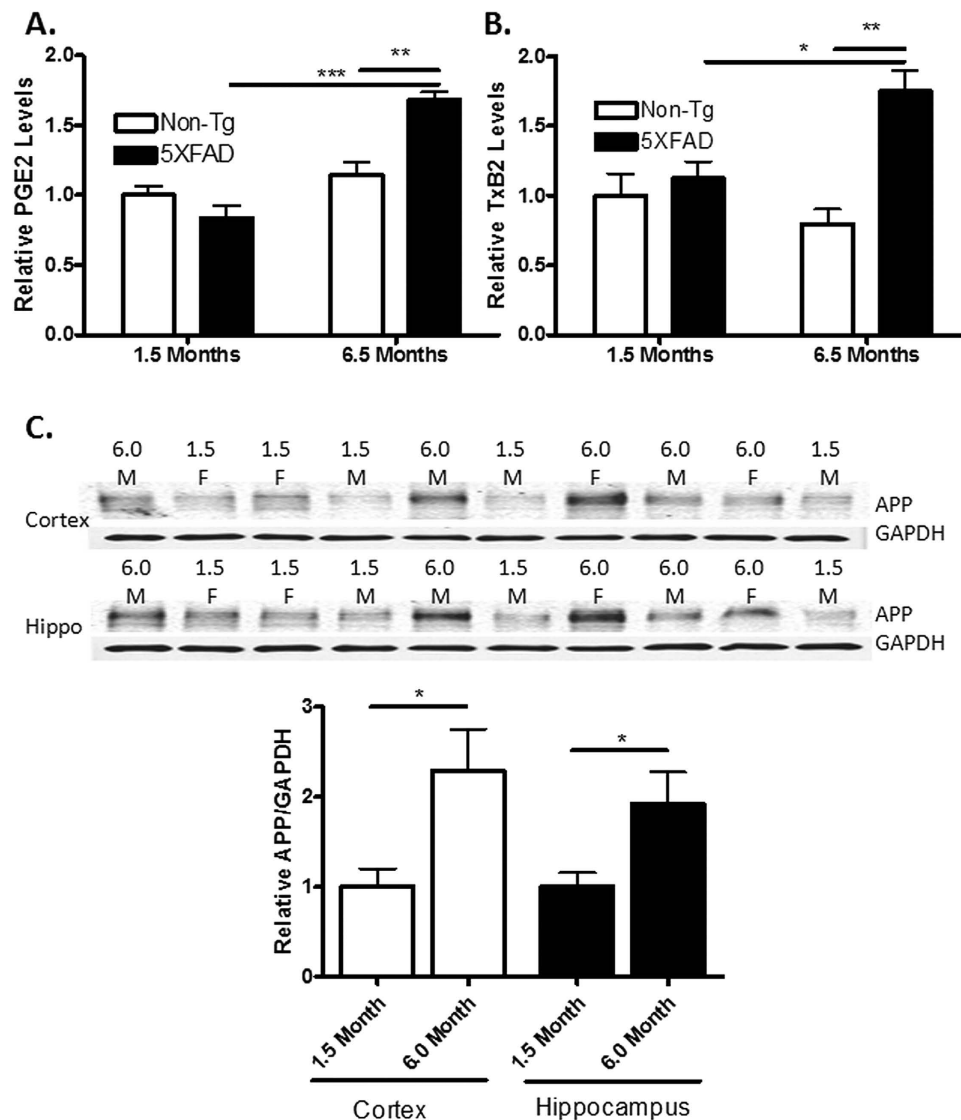


Figure 6. Aged 5XFAD transgenic mice show increased levels of PGE2 and TXB2, as well as APP. Whole hemisphere brain homogenates from 5XFAD mice and non-transgenic (non-Tg) littermates that were 1.5 or 6.5 months of age were analyzed by LC-MS/MS for (A) PGE2 and (B) TXB2 ($n = 3-4$ per group). In (C), the level of total APP expression in cortical and hippocampal brain homogenates from 1.5 month old and 6.0 month old 5XFAD mice was determined by immunoblotting (22C11 antibody), with normalization to GAPDH. Lane loading in the immunoblot was randomized for study blinding during quantification ($n = 5$ per group; 2 females (F) and 3 males (M) in each age group). Statistical analyses consisted of a one-way ANOVA with a Tukey's multiple comparison test for (A) and (B), and a two-tailed t-test in (C). Error bars represent SEM; * $p < 0.05$; ** $p < 0.01$; *** $p < 0.001$.

the enzymes that cleaves APP. A future comparison of APP mRNA levels in young and aged 5XFAD mice would further strengthen this interpretation.

To confirm an involvement of eicosanoids in the regulation of APP in aged 5XFAD mice, we inhibited the key enzymes involved in their synthesis. PG and TX synthesis depends on the metabolic conversion of arachidonic acid to PGH2 by COX-1 and/or COX-2³², and we evaluated known COX inhibitors for their ability to achieve meaningful brain concentrations upon oral administration. Both the selective COX-1 inhibitor, SC-560³³ and the COX-2 inhibitor, rofecoxib³⁴, demonstrated good brain exposures (brain/plasma drug ratios ≥ 0.3) after oral dosing. This led to the administration of a mixture of these two inhibitors in drinking water to 5.5-6-month old 5XFAD mice for 7 days, with a separate group of mice receiving vehicle only. The drug-treated group had appreciable levels of the two compounds in their brains (Supplementary Table 4) that resulted in a nearly complete reduction of PGE2 and TXB2 (Supplementary Figure 5). An evaluation of combined sAPP and intact APP species by immunoblotting with the 22C11 antibody revealed that the COX inhibitors caused a significant reduction of APP levels of approximately 30% within the cortex (Fig. 8A) and hippocampus (Fig. 8B).

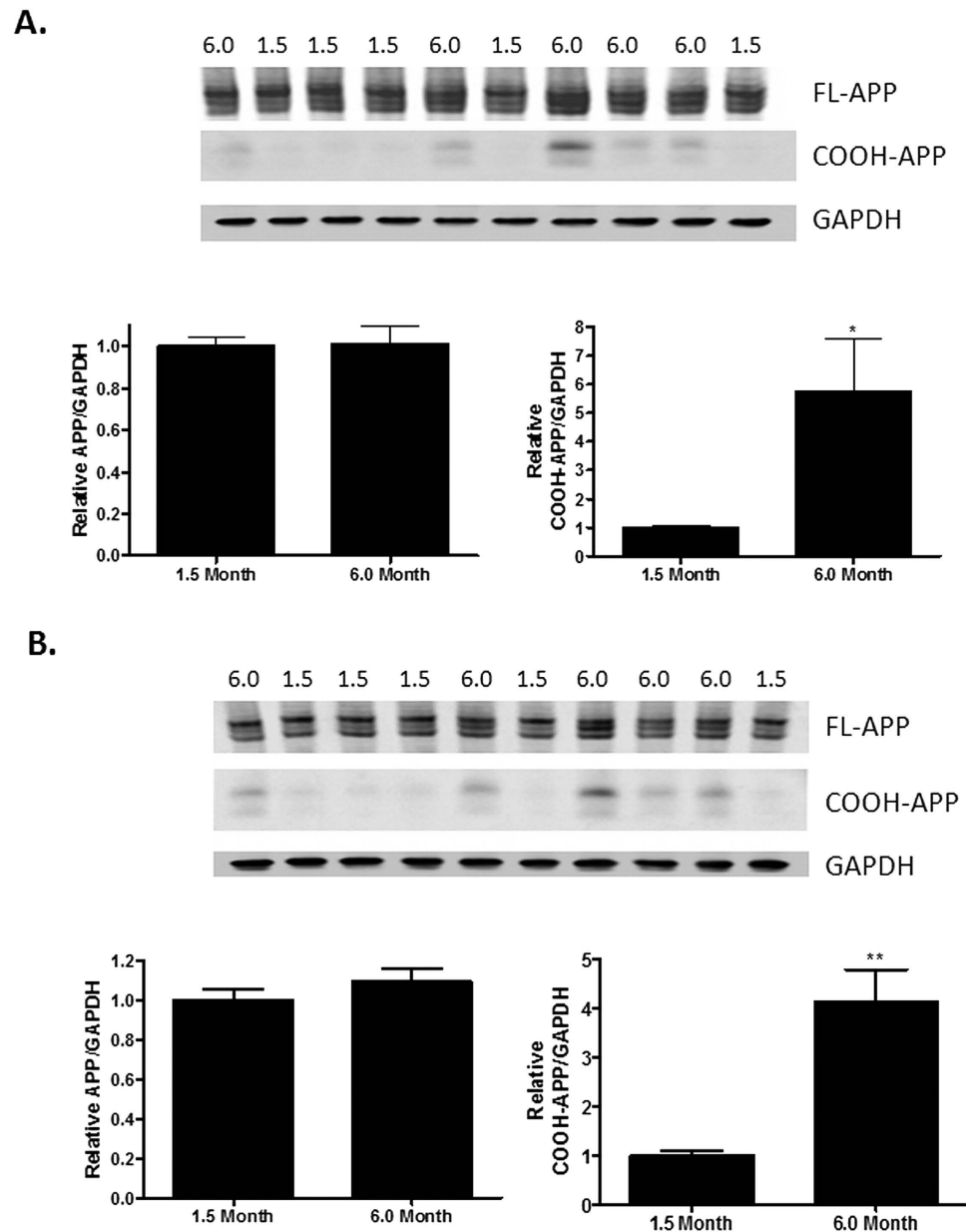


Figure 7. COOH-terminal APP antibody (5685) reveals increased COOH-terminal APP fragments, but not intact APP, in aged 5XFAD mice. APP expression in (A) cortical and (B) hippocampal brain homogenates from 1.5 month old and 6.0 month old 5XFAD mice (same samples as in Fig. 6) was determined by immunoblotting with the COOH-terminal 5685 APP antibody after protein separation on a 4–12% gradient gel, with normalization to GAPDH. Lane loading in the immunoblot was as in Fig. 6. Statistical analyses consisted of a two-tailed t-test $N = 5/\text{group}$; * $p < 0.05$; ** $p < 0.01$.

In addition to the evaluation of COX-derived eicosanoids, a potential role of LTD4 was also investigated through inhibition of 5-LOX, the enzyme responsible for the synthesis of cysLTs³². As LTD4 and related LT levels were found to be below the limit of LC-MS/MS detection, and because a commercial LTB4 ELISA gave artifactual readings from brain homogenates, we could not directly quantify inhibition of 5-LOX activity through the measurement of these species. Thus, we chose to investigate the potential use of the dual COX/5-LOX inhibitor, licoferone³⁵. Although this compound shows poor blood-brain barrier permeability, preliminary studies showed that 0.6 μM brain concentrations could be achieved by administering a high dose (0.7 mg/ml) via drinking water to mice. Importantly, this dose led to ~40–50% reductions in COX activity as assessed by measurements of PGE2 and TXB2 in the brains of aged 5XFAD mice (Supplementary Figure 6). As licoferone has nearly identical IC_{50} values for the inhibition of COX-1, COX-2 and 5-LOX³⁵, a ~40–50% inhibition of 5-LOX should also occur at this dose. Attempts to further increase the licoferone dose to increase 5-LOX inhibition could not be achieved because of compound insolubility. Thus, licoferone was added at 0.7 mg/ml to drinking water containing SC-560 and rofecoxib, which was administered to 5.5–6-month old 5XFAD mice for 7 days. As expected, nearly complete

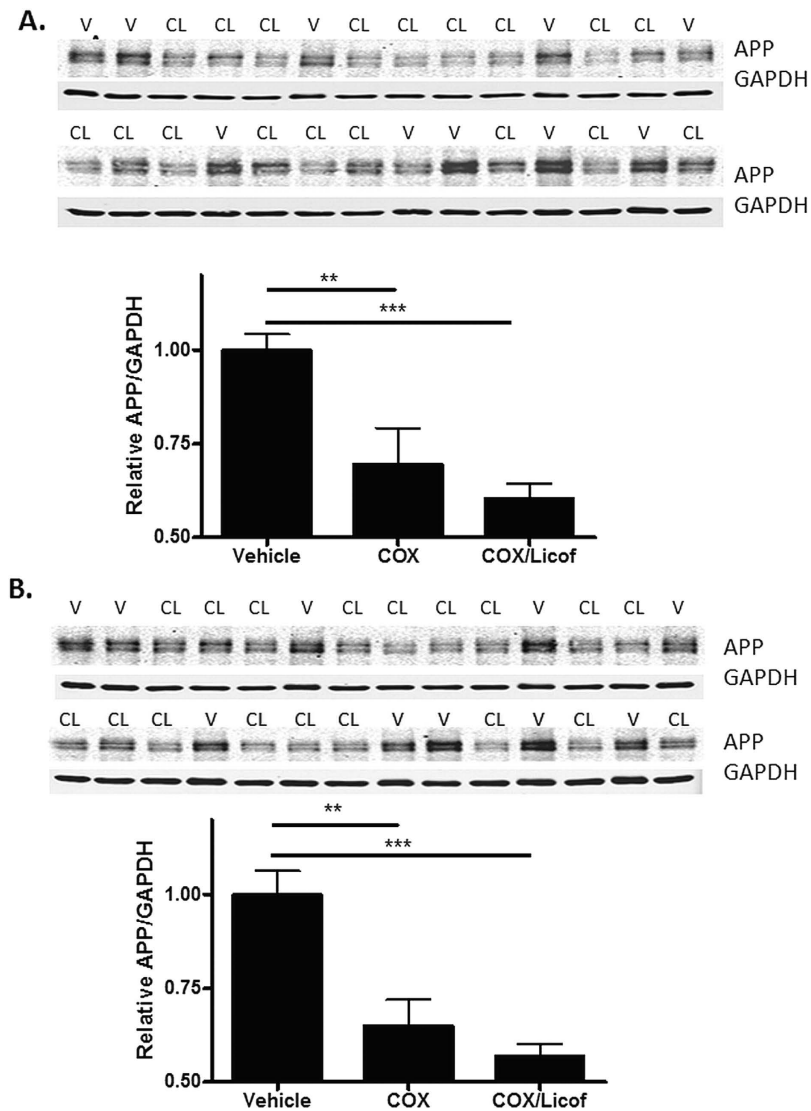


Figure 8. Inhibition of eicosanoid production reduces APP expression in aged 5XFAD transgenic mice. 5XFAD mice (5.5–6.0 months of age) were provided drinking water containing SC-560 and rofecoxib for a total of 7 days (COX group; 3 females and 6 males). Another group of similarly aged 5XFAD mice received the COX inhibitor mixture supplemented with licoferone (COX/Licof group; 5 females and 4 males). A group of age-matched 5XFAD mice received drinking water containing the vehicle only (5 females and 5 males). Quantification of total APP (22C11 antibody) normalized to GAPDH for cortical (A) and hippocampal (B) homogenates revealed a significant reduction in both the COX and COX/Licof treatment groups compared to the vehicle group. Primary immunoblots are shown for the COX/Licof-treated (CL) and vehicle-treated (V) mice, with lane loading randomized for study blinding during quantification. The 9 COX/Licof inhibitor-treated samples were run on each gel, with the 10 vehicle-treated samples split between the two gels. The relative APP/GAPDH value for each drug-treated mouse sample was normalized to the vehicle mean on each gel, with the final APP/GAPDH value consisting of the average sample value derived from the two separate gels. A similar analysis was conducted for the COX inhibitor treatment group. Statistical analyses consisted of a one-way ANOVA with a Tukey's multiple comparison test. * $p < 0.05$; ** $p < 0.01$, *** $p < 0.001$.

inhibition of TXB2 and PGE2 production was observed in the treated mice (Supplementary Figure 5) and 0.6 μ M licoferone levels were again achieved in the brain (Supplementary Table 4), although the mice that received the mixture containing licoferone consumed less water than the groups receiving vehicle or the COX inhibitors only, presumably due to taste aversion since the mice otherwise seemed unaffected, without a significant change in body weight. This resulted in lower SC-560 and rofecoxib brain concentrations than achieved upon treatment with COX inhibitors only (Supplementary Table 4). The addition of licoferone to the COX inhibitors resulted in a greater suppression of APP expression in both the cortex (40%; Fig. 8A) and hippocampus (43%; Fig. 8B) than obtained with the COX inhibitors alone. However, the difference between the COX-only and COX/Licof treatment groups did not reach statistical significance under these conditions of partial 5-LOX inhibition. Thus, although these data

are suggestive, we cannot definitively conclude that the combination of COX and 5-LOX inhibition results in a greater decrease of APP levels than is achieved with COX inhibitors only.

Interestingly, the reduction in total APP upon treatment of the aged 5XFAD mice with inhibitors of eicosanoid synthesis appeared to result from a decrease in sAPP species, as no changes in intact APP were observed when brain samples were analyzed with the COOH-terminal 5685 APP antibody (Supplementary Figure 7). However, there was a significant reduction in COOH-terminal APP fragments in the inhibitor-treated 5XFAD mice, without evidence of a preferential reduction of C99 vs. C83 fragments (Supplementary Figure 7). The coordinate changes in sAPP and COOH-terminal APP fragments are essentially identical to what was observed as the 5XFAD mice aged from 1.5 months to 6.0 months of age. Thus, these data provide further evidence that the increase of APP observed in aged 5XFAD mice results from the age-dependent elevation in eicosanoid levels.

Whereas the reduction of eicosanoids in the aged 5XFAD mice led to a significant diminution of COOH-terminal APP fragments, total A β levels in the brains of these mice did not change after the 7 days of drug treatment (Supplementary Figure 8). As nearly all of the A β in 5XFAD mice of this age is within insoluble plaques, it may not be surprising that a short-term reduction in APP would not lead to meaningful change of total A β . In fact, this result is consistent with what has been observed in APP transgenic mice treated with a potent β -secretase inhibitor³⁶, where reduced A β production did not lead to a significant reduction of total A β after only one week of dosing.

Discussion

There is value in identifying new mechanisms and targets for regulating A β levels in AD brain. In this regard, antagonism of the TP receptor has been suggested as a potential strategy to reduce A β production in AD, as activation of this receptor by iPF2 α III or TXA2 results in increased APP mRNA and APP protein expression, as well as elevated A β release^{11,12}. The TP receptor-mediated increase of APP expression results from mRNA stabilization that does not appear to require 5' - or 3' -untranslated sequences, as this effect can be seen in cellular and animal models utilizing APP transgenes lacking these regions¹¹. We have further investigated the intracellular pathways responsible for TP receptor-mediated elevation of APP, and reveal the involvement of cPKC isoforms that are activated via G α_q -mediated signaling. The observation that the PKC activator, PMA, increased APP and A β production contrasts with earlier studies^{37,38} showing reduced A β release after phorbol ester treatment of APP-expressing cells due to increased α -secretase activity. However, these prior studies examined acute phorbol ester treatment, whereas our studies were performed over a longer treatment period. The data presented here are consistent with a prior report³⁹ of 8 h phorbol ester treatment causing increased APP expression, as well as A β production.

A key finding from our studies that has important implications for AD is the identification of the EP1, EP3 and CysLT1 receptors as additional G α_q -linked GPCRs that can modulate APP and A β expression. This discovery adds to a growing body of evidence implicating glial-derived eicosanoids in AD pathology. For example, genetic knockout of the EP1, EP2 or EP3 receptors has been shown to result in a significant reduction of plaque burden in APP transgenic mice^{40–42} via a number of postulated mechanisms. Similarly, knockout and pharmacological inhibition of the PGE2 EP4 receptor has been reported to reduce plaque burden in an APP Tg mouse model⁴³, although an opposite effect was observed in another APP Tg model⁴⁴. There is also evidence of APP regulation in glia via activation of EP2 receptors^{45,46}. Finally, LTD4 injection into mouse brain was shown to increase expression of APP and A β ⁴⁷, and 5-LOX-derived LTs have also been suggested to contribute to A β plaque deposition through an effect on γ -secretase activity^{48,49}.

The evidence of eicosanoid contribution to A β plaque pathology suggests possible therapeutic strategies to mitigate the effects of these molecules in AD. A dampening of microglial activation might result in the diminished release of these species. However, it could prove difficult to selectively decrease the detrimental aspects of activated microglia without also affecting potential beneficial properties (e.g., A β phagocytosis). An alternative approach could be antagonism of eicosanoid receptors, but the evidence implicating multiple neuronal eicosanoid receptors as contributing to the regulation of APP expression and A β production presents a multi-target pharmacological challenge. Nonetheless, there may be merit in further exploration of this strategy, as selective antagonism of the most detrimental eicosanoid receptor(s) could provide an effective therapeutic strategy.

Perhaps the most straightforward potential therapeutic strategy to prevent the eicosanoid-driven increases of APP and A β in AD would be through inhibition of eicosanoid production, an approach that has been explored with varying results. COX inhibitors have been shown to fairly consistently reduce A β pathology in several AD mouse models, although negative reports exist^{33,50,51} and in some instances reduction of plaques may have resulted in whole or part from the ability of certain non-steroidal anti-inflammatory drugs (NSAIDs), such as ibuprofen, to modulate γ -secretase activity^{52,53}. Moreover, although multiple epidemiological studies suggest that non-steroidal anti-inflammatory drug (NSAID) regimens can reduce the incidence of AD^{51,54}, NSAIDs have not generally proven effective in AD clinical trials^{55–57}. There are possible explanations for this lack of clinical success. For example, several of the trials utilized COX-2-selective agents, and it may be COX-1 that is up-regulated upon glial activation in AD^{33,51}. In this regard, asymptomatic individuals treated with the dual COX-1/COX-2 inhibitor naproxen showed some evidence of reduced AD onset 2–3 years after completion of the ADAPT trial, whereas those receiving a COX-2 selective agent did not⁵⁸. Moreover, it is possible that COX inhibition alone may lead to shunting of arachidonic acid to the 5-LOX pathway, resulting in increased production of LTs^{59,60}. This might cause CysLT1 receptor activation and increased APP and A β levels, as well as increased A β via enhanced γ -secretase cleavage of APP^{48,49}. Thus, the utilization of a combination of COX and 5-LOX inhibitors, or dual-acting COX/5-LOX inhibitors⁶¹, may merit consideration for AD. It has been reported that 5-LOX and COX levels are increased in the AD brain^{32,48,62,63}, and combined COX/5-LOX inhibitors should reduce the production of PGs, TXs and LTs. Furthermore, whereas NSAIDs can cause gastrointestinal or cardiovascular complications, and were poorly tolerated by a percentage of AD patients⁶⁴, dual COX/5-LOX inhibitors such as licofelone appear to have decreased

side-effects when compared to typical NSAIDs^{35,65}. Thus, there would appear to be merit in evaluating the effects of prolonged inhibition of both COX and 5-LOX enzymes in APP Tg mouse models of plaque formation to test this therapeutic strategy. However, such an approach would result in a systemic reduction of PGs, TXs and LTs, some of which clearly play a beneficial role within the body, so as with all drugs, a benefit-to-risk assessment would be important if such a strategy were pursued.

In summary, our studies further elucidate how inflammatory eicosanoids might contribute to AD pathogenesis, and provide important new information about GPCR regulation of APP expression. The approximately two-fold increase of APP levels that are observed in culture systems upon activation of the multiple G_{α_q} -linked eicosanoid receptors described herein is consistent with reports of elevated APP in AD brain^{66,67}, as well as the increased APP expression that we observed in plaque-bearing 5XFAD mice. These observations suggest that initial $A\beta$ plaque formation and glial activation in the brain results in the initiation of a vicious cycle, whereby glial-derived eicosanoids may further elevate APP and $A\beta$ expression, thereby accelerating additional plaque deposition. Our data showing that inhibition of eicosanoid synthesis decreases total APP levels and reduces COOH-terminal APP fragments in aged 5XFAD mice supports this cascade hypothesis, and provide impetus to further investigate the contribution of these inflammatory molecules and their receptors to $A\beta$ plaque pathology.

Methods

Cell culture and transfection. QBI293 cells expressing hTP and/or hAPP¹² were grown in DMEM cell culture plus 10% FBS and 1% pen/strep at 37 °C with 5% CO₂. For studies utilizing siRNA, cells in 6-well plates were transfected with 30–50 nM siRNA via Lipofectamine RNAiMax reagent according to the manufacturer's protocol (Life Technologies; Grand Island, NY) 18–24 h prior to any subsequent treatment. The following siRNAs were used: Cntl, G_{α_q} and PKC β siRNA (Santa Cruz Biotechnologies, Inc.; Dallas, TX); $G_{\alpha_{12}}$ and $G_{\alpha_{13}}$ (Thermo Scientific; Waltham, MA); and PKC ϵ and PKC α (Qiagen; Hilden, Germany). For transfection of GPCRs, 5 μ g of cDNA for the human EP1 receptor (Missouri S&T cDNA Resource Center; Rolla, MO) or human EP3, CysLT1, and BLT1 receptors (Origene; Rockville, MD) was introduced into QBI293 cells stably expressing hAPP₆₉₅ using Lipofectamine 2000 (Life Technologies; Grand Island, NY) in 70% confluent 10 cm dishes. Cells were replated into 6-well culture plates and treated as indicated after adhering to the plates. Primary hippocampal neurons from embryonic Sprague Dawley rats or cortical neurons from embryonic CD1 mice were obtained from a core facility (University of Pennsylvania; Philadelphia, PA). The neurons were cultured in 1xNeurobasal A medium with B27 and penicillin/streptomycin (Life Technologies, Grand Island, NY). Mouse neuron medium was also supplemented with 1xGlutamax (Life Technologies, Grand Island, NY). All neuronal cultures had 2.3 μ M cytosine arabinoside (Sigma-Aldrich, St. Louis, MO) added starting 2 days after plating to inhibit the proliferation of mitotic cells (largely astrocytes), and the cultures were allowed to grow 14–16 days prior to treatment. QBI293 cells or neurons were treated as indicated in the figure legends with IBOP, LTD4, LTB4 (Cayman Chemical Company, Inc.; Ann Arbor, MI); 17PGE2 (Santa Cruz, Biotechnologies, Inc.; Dallas, TX); and/or PMA, ionomycin, Y-27632, and Go6983 (Sigma-Aldrich; St. Louis, MO).

RNA isolation and qRT-PCR. Cells were washed, lysed, and RNA was isolated according to the RNEasy manufacturer's protocol (Qiagen; Hilden, Germany). RNA (3 μ g) was converted to cDNA using SuperScript III Reverse Transcriptase (Life Technologies; Grand Island, NY). For RT-PCR, the cDNA was diluted 1:8 in water and 7.6 μ L of the product was added to each well containing SYBR Green Master Mix (Life Technologies; Grand Island, NY) and forward and reverse primers at a final concentration that was determined to yield the greatest amplification efficiency (100 nM for APP and 300 nM for all other primer sets). qRT-PCR was run on the Applied Biosystems 7500 Fast Real-time PCR system (Life Technologies; Grand Island, NY) using the $\Delta\Delta C_t$ comparative method of the analyzed gene product vs. GAPDH. The sequences of the primers used for qRT-PCR analysis are shown in Table 1.

	Sense	Antisense
hG α_q	CATCAATGGGTCAGGATACTCTGATGAAG	GTGCATGAGCCTTATTGTGCTCATAC
hG α_{12}	CAAGGGCTCAAGGGTTCTTGTTG	CTGATGCCAGAATCCCTCCAGA
hG α_{13}	CTGGTGAAGATCCTGCTGCTGG	CCAGCACCCATACACCTTTGATCAC
hAPP	CCAACCAAGTACCATCCAGAACTG	GCACTTGTGAGGAAACGAGAAGGG
hGAPDH	GAAGGTGAAGGTCGGAGTCAACG	CCAGAGTAAAAGCAGCCCTGGTG
hPKC α	CCACCATTCAAGCCCAAAGTGTG	GGCTGTCTCGTGTGTGAAGAAC
hPKC ϵ	GCTTGAAGCCACAGCCTG	CTTGTGGCCGTTGACCTGATG
hPKC β II	GGATTGGGAGAACTTGAACGCAAAGAG	CCTGATGACTTCTGGTCGGG
hTP	ACGGAGAAGGAGCTGCTCATC	GCGGCGAACAGGATATACA
hEP1	CCTGTGCGTATCATGGTGGTGTGTC	GCTTACCGGAAGTGGCTGAGG
hEP3	AAGGCCACGGCATCTCAGT	TGATCCCATAAGCTGAATGG
hCysLT1	GAGAAACATGGATGAAACAGGAAATCTGACAG	CAAAGCATAGGTGCTGAGGCG
hBLT1	GTCTGCGGAGTCAGCATTGTACG	GTAGCCGACGCCATATGTCC

Table 1. qPCR primer pairs.

Immunoblot analysis. Cells were lysed in RIPA buffer (50 mM Tris, 150 mM NaCl, 0.5% sodium deoxycholate, 0.1% SDS, 1% NP-40, 5 mM EDTA, pH 8.0) containing a protease inhibitor cocktail (Sigma-Aldrich; St. Louis, MO) and 2 mM PMSF. Lysate was vortexed and then centrifuged at 13,000 \times g at 4 °C for 30 min. For examination of APP levels in brains of 5XFAD transgenic mice, cortex and hippocampus were removed from freshly dissected brains obtained from mice euthanized according to protocols approved by the Institutional Animal Care and Use Committee (IACUC). The samples were quick frozen on dry ice, and subsequently homogenized and sonicated in 2% SDS containing the protease inhibitor cocktail and 2 mM PMSF. The homogenates were centrifuged at 40,000 \times g for 30 min at room temperature. The supernatants were collected and the pellets were again sonicated in 2% SDS containing protease inhibitors and 2 mM PMSF. After another centrifugation at 40,000 \times g for 30 min at room temperature, the supernatant was combined with the initial supernatant. The total protein concentration of cell- or brain-derived samples was determined by BCA assay (Pierce Biotechnologies; Rockford, IL). For most analyses, proteins were separated on 10% SDS-PAGE gels, transferred to nitrocellulose membranes, blocked in blocking buffer (LiCor Biosciences; Lincoln, NE), and incubated overnight with one of the following primary antibodies: APP (amino-terminal, 22C11⁶⁸ and Karen⁶⁹; carboxyl-terminal, 5685³¹); α -tubulin (Covance; Princeton, NJ); GAPDH (Millipore; Billerica, MA); G α_q , G α_{12} , PKC ϵ (Santa Cruz Biotechnologies, Inc.; Dallas, TX); G α_{13} (AbCam; Cambridge, MA); or PKC α (Cell signaling; Danvers, MA). Membranes were washed 3 times for 10 min in Tris-buffered saline and incubated with IRDye 800CW- or 680RD-conjugated 2° antibodies, followed by imaging and quantification with the Odyssey Imaging System (LI-COR Biosciences; Lincoln, NE). For the analysis of APP and COOH-terminal APP fragments, proteins were separated on 4–12% Bis-Tris gradient gels with MES running buffer (Life Technologies, Grand Island, NY), transferred to nitrocellulose membranes, blocked in 5% milk and incubated overnight with the 5685 APP carboxyl-terminal antibody, followed by treatment with 2° antibodies as above. Membranes of transfers from 10% gels were routinely cut between the 50 kD and 75 kD molecular weight markers prior to primary antibody incubations so as to allow for independent staining of APP species and house-keeping genes. For studies with 5XFAD transgenic mice, the identity of brain samples were masked prior to gel loading so that the individual conducting immunoblot quantification was unaware of the lane assignments.

A β 40 and A β 42 ELISA. A β 1-40 and A β 1-42 levels were determined by ELISA as previously described¹². In 2% SDS cortical homogenates from vehicle- or drug-treated 5XFAD mice, the samples were diluted at least 100-fold, such that the final readings fell within the linear portion of a standard curve.

COX and 5-LOX Inhibitor Administration to 5XFAD Transgenic Mice. All mouse studies were approved by the University of Pennsylvania IACUC. Male and female 5XFAD transgenic mice³⁰ were utilized in these studies, with the age of the mice, the number of mice per group, and their gender distribution listed in the figure legends. The 5XFAD mice express human APP and PS1 that contain 5 mutations associated with familial AD, with germ-line transmission and stable genomic cointegration of both transgenes³⁰. Heterozygous male 5XFAD mice (B6/SJL background) were bred with B6/SJL F1 hybrids, and transgenic mice were identified by PCR analysis of tail clips using primers specific for the human APP and human PS1 transgenes. Only mice that were positive for both transgenes were classified as 5XFAD transgenics. Mice from different breedings were grouped together to obtain sufficient group sizes that were within 2 weeks of age. Aged 5XFAD mice were administered either a combination of SC-560 and rofecoxib, a mixture of SC-560, rofecoxib, and licofelone, or vehicle alone for 7 days via drinking water. SC-560 and rofecoxib were formulated at 70 μ g/mL each, and licofelone at 0.7 mg/ml, in 3% (v/v) polyethylene glycol 400, 0.5% (w/v) methyl cellulose 400 cP and 10% (w/v) sucrose. The mice were given *ad libitum* access to the water.

Quantification of TXB2 and PGE2 in Brain Extracts. PGE2 and TXB2 were extracted from mouse brain homogenates and quantified using stable isotope dilution (SID) LC-MS/MS. Mouse brain hemispheres were homogenized in 10 mM ammonium acetate buffer pH 5.8 (50% w/v) and extracted essentially as described⁷⁰. Briefly, 3 ml of an acetone/saline solution (2:1) with 0.01% butylated hydroxytoluene (BHT) as an antioxidant was added to 0.1 mL (50 mg) of brain homogenate that had been spiked with 1 ng PGE2-d4 and 1 ng TXB2-d4. This mixture was vortexed for 4 min and then centrifuged at 2000 \times g for 10 min. The supernatant was moved to a new tube and 2 ml of hexane was added. After 1 min of vortex mixing and centrifugation as above, the upper hexane phase was discarded. The lower phase was acidified with 30 μ l of 2M acetic acid, followed by the addition of 2 ml of chloroform containing 0.01% BHT. This mixture was vortexed, centrifuged as above, and the lower chloroform phase dried under nitrogen in a 35 °C water bath. Dried samples were reconstituted in 0.1 ml of ethanol for subsequent analysis by LC-MS/MS (Acquity UPLC-TQD; Waters Corporation, Milford, MA, USA). Samples (10 μ L) were separated on a BEH C18 column (1.7 μ m, 2.1 \times 50 mm) using a water/acetonitrile gradient with 0.1% formic acid from 5 to 95% acetonitrile over 5 minutes at 0.6 mL/min and 35 °C. Compounds were detected in negative electrospray ionization mode. Source voltages and MS parameters were optimized for PGE2 and TXB2 during direct infusion of standard solutions (Cayman Chemical, Ann Arbor, MI). Analytes and standards were detected using multiple reaction monitoring of their specific collision induced ion transitions as follows (negative *m/z*): PGE2 (351 > 271), PGE2-d4 (355 > 275), TXB2 (369 > 169), TXB2-d4 (373 > 173). Standard solutions were prepared with a constant 1 ng of deuterium-labeled internal standard and varying amounts of analyte over concentrations from 1 to 1000 ng/mL. Peak area ratios (analyte/internal standard) were plotted versus standard concentration and a linear regression curve was fit to the data.

Statistics. Linear mixed-effect models were used to compare the outcomes in cell culture studies when there were three or more treatment groups. The fixed-effects in the linear mixed-effects model were the treatment types and replicate runs, whereas experiment-specific random intercepts were used to account for the correlation

between repeated measures within an experiment. Analyses were conducted with SAS v.9.2 (SAS Institute, Inc., Cary, NC). All statistics were two-tailed, with $P \leq 0.05$ considered significant. For cell culture or mouse experiments in which only two treatment types were compared, statistical analysis consisted of an unpaired, two-tailed T-test (GraphPad Prism, GraphPad Software, La Jolla, CA). For mouse studies in which three or more treatment conditions were compared, an ANOVA analysis was conducted with either a Dunnett's or Tukey's post-hoc multiple comparison test (GraphPad Prism, GraphPad Software, La Jolla, CA). Detailed statistical outcomes are provided in the Supplementary Materials.

References

- Selkoe, D. J. & Schenk, D. Alzheimer's disease: Molecular understanding predicts amyloid-based therapeutics. *Annual Review of Pharmacology and Toxicology* **43**, 545–584 (2003).
- Karran, E., Mercken, M. & De Strooper, B. The amyloid cascade hypothesis for Alzheimer's disease: an appraisal for the development of therapeutics. *Nature Reviews. Drug Discovery* **10**, 698–712 (2011).
- Lee, V. M. Y., Goedert, M. & Trojanowski, J. Q. Neurodegenerative tauopathies. *Annual Review of Neuroscience* **24**, 1121–1159 (2001).
- Sultana, R. & Butterfield, D. A. Role of oxidative stress in the progression of Alzheimer's disease. *J Alzheimers Dis* **19**, 341–353 (2010).
- Wyss-Coray, T. & Rogers, J. Inflammation in Alzheimer disease—a brief review of the basic science and clinical literature. *Cold Spring Harbor Perspectives in Medicine* **2**, a006346 (2012).
- Haga, S., Akai, K. & Ishii, T. Demonstration of microglial cells in and around senile (neuritic) plaques in the Alzheimer brain. An immunohistochemical study using a novel monoclonal antibody. *Acta Neuropathol* **77**, 569–575 (1989).
- Rogers, J., Lubner-Narod, J., Styren, S. D. & Civin, W. H. Expression of immune system-associated antigens by cells of the human central nervous system: relationship to the pathology of Alzheimer's disease. *Neurobiol Aging* **9**, 339–349 (1988).
- Dumont, M. & Beal, M. F. Neuroprotective strategies involving ROS in Alzheimer disease. *Free Radical Biology & Medicine* **51**, 1014–1026 (2011).
- Montine, T. J., Markesbery, W. R., Morrow, J. D. & Roberts, L. J., 2nd. Cerebrospinal fluid F2-isoprostane levels are increased in Alzheimer's disease. *Ann Neurol* **44**, 410–413 (1998).
- Pratico, D., Lee, V., Trojanowski, J. Q., Rokach, J. & Fitzgerald, G. A. Increased F2-isoprostanes in Alzheimer's disease: evidence for enhanced lipid peroxidation *in vivo*. *FASEB Journal: Official Publication of the Federation of American Societies for Experimental Biology* **12**, 1777–1783 (1998).
- Shineman, D. W., Zhang, B., Leight, S. N., Pratico, D. & Lee, V. M. Y. Thromboxane receptor activation mediates isoprostane-induced increases in amyloid pathology in Tg2576 mice. *Journal of Neuroscience* **28**, 4785–4794 (2008).
- Soper, J. H. *et al.* Brain-penetrant tetrahydronaphthalene thromboxane A2-prostanoid (TP) receptor antagonists as prototype therapeutics for Alzheimer's disease. *ACS Chemical Neuroscience* **3**, 928–940 (2012).
- Giulian, D., Corpuz, M., Richmond, B., Wendt, E. & Hall, E. R. Activated microglia are the principal glial source of thromboxane in the central nervous system. *Neurochemistry International* **29**, 65–76 (1996).
- Klegeris, A. & McGeer, P. L. Toxicity of human monocytic THP-1 cells and microglia toward SH-SY5Y neuroblastoma cells is reduced by inhibitors of 5-lipoxygenase and its activating protein FLAP. *Journal of Leukocyte Biology* **73**, 369–378 (2003).
- Combrinck, M. *et al.* Levels of CSF prostaglandin E2, cognitive decline, and survival in Alzheimer's disease. *Journal of Neurology, Neurosurgery, and Psychiatry* **77**, 85–88 (2006).
- Montine, T. J. *et al.* Elevated CSF prostaglandin E2 levels in patients with probable AD. *Neurology* **53**, 1495–1498 (1999).
- Nakahata, N. Thromboxane A2: physiology/pathophysiology, cellular signal transduction and pharmacology. *Pharmacology & Therapeutics* **118**, 18–35 (2008).
- Young, L. H., Balin, B. J. & Weis, M. T. Go 6983: a fast acting protein kinase C inhibitor that attenuates myocardial ischemia/reperfusion injury. *Cardiovascular Drug Reviews* **23**, 255–272 (2005).
- Narumiya, S., Ishizaki, T. & Uehata, M. Use and properties of ROCK-specific inhibitor Y-27632. *Methods in Enzymology* **325**, 273–284 (2000).
- Paul, B. Z., Daniel, J. L. & Kunapuli, S. P. Platelet shape change is mediated by both calcium-dependent and -independent signaling pathways. Role of p160 Rho-associated coiled-coil-containing protein kinase in platelet shape change. *J Biol Chem* **274**, 28293–28300 (1999).
- Mochly-Rosen, D., Das, K. & Grimes, K. V. Protein kinase C, an elusive therapeutic target? *Nature Reviews. Drug Discovery* **11**, 937–957 (2012).
- Castagna, M. *et al.* Direct activation of calcium-activated, phospholipid-dependent protein kinase by tumor-promoting phorbol esters. *J Biol Chem* **257**, 7847–7851 (1982).
- Liu, C. & Hermann, T. E. Characterization of ionomycin as a calcium ionophore. *J Biol Chem* **253**, 5892–5894 (1978).
- Wei, L. L. *et al.* Roles of the prostaglandin E2 receptors EP subtypes in Alzheimer's disease. *Neuroscience Bulletin* **26**, 77–84 (2010).
- Fang, S. H. *et al.* Increased expression of cysteinyl leukotriene receptor-1 in the brain mediates neuronal damage and astrogliosis after focal cerebral ischemia in rats. *Neuroscience* **140**, 969–979 (2006).
- Okubo, M., Yamanaka, H., Kobayashi, K. & Noguchi, K. Leukotriene synthases and the receptors induced by peripheral nerve injury in the spinal cord contribute to the generation of neuropathic pain. *Glia* **58**, 599–610 (2010).
- Bernstein, P. R. Chemistry and structure–activity relationships of leukotriene receptor antagonists. *American Journal of Respiratory and Critical Care Medicine* **157**, S220–225 (1998).
- Watanabe, K. *et al.* Role of the prostaglandin E receptor subtype EP1 in colon carcinogenesis. *Cancer Res* **59**, 5093–5096 (1999).
- Juteau, H. *et al.* Structure–activity relationship on the human EP3 prostanoid receptor by use of solid-support chemistry. *Bioorg Med Chem Lett* **11**, 747–749 (2001).
- Oakley, H. *et al.* Intraneuronal beta-amyloid aggregates, neurodegeneration, and neuron loss in transgenic mice with five familial Alzheimer's disease mutations: potential factors in amyloid plaque formation. *J Neurosci* **26**, 10129–10140 (2006).
- Lee, E. B. *et al.* BACE overexpression alters the subcellular processing of APP and inhibits Abeta deposition *in vivo*. *The Journal of Cell Biology* **168**, 291–302 (2005).
- Manev, H., Chen, H., Dzitoyeva, S. & Manev, R. Cyclooxygenases and 5-lipoxygenase in Alzheimer's disease. *Progress in Neuro-Psychopharmacology & Biological Psychiatry* **35**, 315–319 (2011).
- Choi, S. H. *et al.* Cyclooxygenase-1 inhibition reduces amyloid pathology and improves memory deficits in a mouse model of Alzheimer's disease. *J Neurochem* **124**, 59–68 (2013).
- Warner, T. D. & Mitchell, J. A. Cyclooxygenases: new forms, new inhibitors, and lessons from the clinic. *FASEB J* **18**, 790–804 (2004).
- Kulkarni, S. K. & Singh, V. P. Licofelone: the answer to unmet needs in osteoarthritis therapy? *Current Rheumatology Reports* **10**, 43–48 (2008).
- Eketjall, S. *et al.* AZ-4217: a high potency BACE inhibitor displaying acute central efficacy in different *in vivo* models and reduced amyloid deposition in Tg2576 mice. *J Neurosci* **33**, 10075–10084 (2013).
- Buxbaum, J. D. *et al.* Cholinergic agonists and interleukin 1 regulate processing and secretion of the Alzheimer beta/A4 amyloid protein precursor. *Proceedings of the National Academy of Sciences of the United States of America* **89**, 10075–10078 (1992).

38. Yeon, S. W. *et al.* Blockade of PKC epsilon activation attenuates phorbol ester-induced increase of alpha-secretase-derived secreted form of amyloid precursor protein. *Biochemical and Biophysical Research Communications* **280**, 782–787 (2001).
39. da Cruz e Silva, O. A. *et al.* Enhanced generation of Alzheimer's amyloid-beta following chronic exposure to phorbol ester correlates with differential effects on alpha and epsilon isozymes of protein kinase C. *Journal of Neurochemistry* **108**, 319–330 (2009).
40. Zhen, G. *et al.* PGE2 EP1 receptor exacerbated neurotoxicity in a mouse model of cerebral ischemia and Alzheimer's disease. *Neurobiol Aging* **33**, 2215–2219 (2012).
41. Shi, J. *et al.* Inflammatory prostaglandin E2 signaling in a mouse model of Alzheimer disease. *Ann Neurol* **72**, 788–798 (2012).
42. Liang, X. *et al.* Deletion of the prostaglandin E2 EP2 receptor reduces oxidative damage and amyloid burden in a model of Alzheimer's disease. *J Neurosci* **25**, 10180–10187 (2005).
43. Hoshino, T. *et al.* Improvement of cognitive function in Alzheimer's disease model mice by genetic and pharmacological inhibition of the EP(4) receptor. *J Neurochem* **120**, 795–805 (2012).
44. Woodling, N. S. *et al.* Suppression of Alzheimer-associated inflammation by microglial prostaglandin-E2 EP4 receptor signaling. *J Neurosci* **34**, 5882–5894 (2014).
45. Lee, R. K., Knapp, S. & Wurtman, R. J. Prostaglandin E2 stimulates amyloid precursor protein gene expression: inhibition by immunosuppressants. *J Neurosci* **19**, 940–947 (1999).
46. Pooler, A. M., Arjona, A. A., Lee, R. K. & Wurtman, R. J. Prostaglandin E2 regulates amyloid precursor protein expression via the EP2 receptor in cultured rat microglia. *Neurosci Lett* **362**, 127–130 (2004).
47. Tang, S. S. *et al.* Leukotriene D4 induces cognitive impairment through enhancement of CysLT(1) R-mediated amyloid-beta generation in mice. *Neuropharmacology* **65**, 182–192 (2013).
48. Firuzi, O., Zhuo, J., Chinnici, C. M., Wisniewski, T. & Pratico, D. 5-Lipoxygenase gene disruption reduces amyloid-beta pathology in a mouse model of Alzheimer's disease. *FASEB J* **22**, 1169–1178 (2008).
49. Chu, J. & Pratico, D. Pharmacologic blockade of 5-lipoxygenase improves the amyloidotic phenotype of an Alzheimer's disease transgenic mouse model involvement of gamma-secretase. *The American Journal of Pathology* **178**, 1762–1769 (2011).
50. Hillmann, A. *et al.* No improvement after chronic ibuprofen treatment in the 5XFAD mouse model of Alzheimer's disease. *Neurobiol Aging* **33**, 833 e839–850 (2012).
51. McGeer, P. L. & McGeer, E. G. NSAIDs and Alzheimer disease: epidemiological, animal model and clinical studies. *Neurobiol Aging* **28**, 639–647 (2007).
52. Kukar, T. *et al.* Diverse compounds mimic Alzheimer disease-causing mutations by augmenting Abeta42 production. *Nat Med* **11**, 545–550 (2005).
53. Weggen, S. *et al.* A subset of NSAIDs lower amyloidogenic Abeta42 independently of cyclooxygenase activity. *Nature* **414**, 212–216 (2001).
54. Szekely, C. A. *et al.* Nonsteroidal anti-inflammatory drugs for the prevention of Alzheimer's disease: a systematic review. *Neuroepidemiology* **23**, 159–169 (2004).
55. Leoutsakos, J. M., Muthen, B. O., Breitner, J. C. & Lyketsos, C. G. Effects of non-steroidal anti-inflammatory drug treatments on cognitive decline vary by phase of pre-clinical Alzheimer disease: findings from the randomized controlled Alzheimer's Disease Anti-inflammatory Prevention Trial. *International Journal of Geriatric Psychiatry* **27**, 364–374 (2012).
56. Martin, B. K. *et al.* Cognitive function over time in the Alzheimer's Disease Anti-inflammatory Prevention Trial (ADAPT): results of a randomized, controlled trial of naproxen and celecoxib. *Arch Neurol* **65**, 896–905 (2008).
57. Szekely, C. A. *et al.* No advantage of A beta 42-lowering NSAIDs for prevention of Alzheimer dementia in six pooled cohort studies. *Neurology* **70**, 2291–2298 (2008).
58. Breitner, J. C. *et al.* Extended results of the Alzheimer's disease anti-inflammatory prevention trial. *Alzheimer's & Dementia: the Journal of the Alzheimer's Association* **7**, 402–411 (2011).
59. Maxis, K. *et al.* The shunt from the cyclooxygenase to lipoxygenase pathway in human osteoarthritic subchondral osteoblasts is linked with a variable expression of the 5-lipoxygenase-activating protein. *Arthritis Research & Therapy* **8**, R181 (2006).
60. Duffield-Lillico, A. J. *et al.* Levels of prostaglandin E metabolite and leukotriene E(4) are increased in the urine of smokers: evidence that celecoxib shunts arachidonic acid into the 5-lipoxygenase pathway. *Cancer Prevention Research* **2**, 322–329 (2009).
61. Hwang, S. H. W., Weckler, A. T., Wagner, K. & Hammock, B. D. Rationally designed multitarget agents against inflammation and pain. *Curr Med Chem* **20**, 1783–1799 (2013).
62. Kitamura, Y. *et al.* Increased expression of cyclooxygenases and peroxisome proliferator-activated receptor-gamma in Alzheimer's disease brains. *Biochem Biophys Res Commun* **254**, 582–586 (1999).
63. Fujimi, K. *et al.* Altered expression of COX-2 in subdivisions of the hippocampus during aging and in Alzheimer's disease: the Hisayama Study. *Dementia and Geriatric Cognitive Disorders* **23**, 423–431 (2007).
64. Montine, T. J., Sonnen, J. A., Milne, G., Baker, L. D. & Breitner, J. C. Elevated ratio of urinary metabolites of thromboxane and prostacyclin is associated with adverse cardiovascular events in ADAPT. *PLoS one* **5**, e9340 (2010).
65. Brune, K. Safety of anti-inflammatory treatment--new ways of thinking. *Rheumatology* **43**Suppl 1, i16–20 (2004).
66. Vitek, M. P. Increasing amyloid peptide precursor production and its impact on Alzheimer's disease. *Neurobiology of Aging* **10**, 471–473 (1989).
67. Palmert, M. R. *et al.* Amyloid protein precursor messenger RNAs: differential expression in Alzheimer's disease. *Science* **241**, 1080–1084 (1988).
68. Weidemann, A. *et al.* Identification, biogenesis, and localization of precursors of Alzheimer's disease A4 amyloid protein. *Cell* **57**, 115–126 (1989).
69. Turner, R. S., Suzuki, N., Chyung, A. S., Younkin, S. G. & Lee, V. M. Amyloids beta40 and beta42 are generated intracellularly in cultured human neurons and their secretion increases with maturation. *J Biol Chem* **271**, 8966–8970 (1996).
70. Golovko, M. Y. & Murphy, E. J. An improved LC-MS/MS procedure for brain prostanoic acid analysis using brain fixation with head-focused microwave irradiation and liquid-liquid extraction. *Journal of Lipid Research* **49**, 893–902 (2008).

Acknowledgements

We thank Drs. Virginia M-Y. Lee and John Q. Trojanowski for generously sharing resources and for their critical reading of the manuscript. We also thank Drs. Linda Kwong, Kelvin Luk and Hugo Geerts for their review of the manuscript, Xiaoyan Han for statistical programming support, and Dr. Robert Vassar for providing 5XFAD transgenic mice to the Center for Neurodegenerative Disease Research at the University of Pennsylvania. This work was funded by NIH grant R01AG034140. Dr. Sharon Xie's effort is supported by NIH grant AG10124.

Author Contributions

L.L., M.J. and Y.Y. all contributed experimentally to the manuscript. S.X.X. provided statistical advice and conducted mixed-effects model statistical analyses. K.H.-R. contributed experimentally, in study design and in the preparation of the manuscript. K.B. contributed to the study conception, study design, data review and manuscript preparation.

Additional Information

Supplementary information accompanies this paper at <http://www.nature.com/srep>

Competing financial interests: The authors declare no competing financial interests.

How to cite this article: Herbst-Robinson, K. J. *et al.* Inflammatory Eicosanoids Increase Amyloid Precursor Protein Expression via Activation of Multiple Neuronal Receptors. *Sci. Rep.* **5**, 18286; doi: 10.1038/srep18286 (2015).



This work is licensed under a Creative Commons Attribution 4.0 International License. The images or other third party material in this article are included in the article's Creative Commons license, unless indicated otherwise in the credit line; if the material is not included under the Creative Commons license, users will need to obtain permission from the license holder to reproduce the material. To view a copy of this license, visit <http://creativecommons.org/licenses/by/4.0/>